DO-TH/04-05

DELINEATING THE (UN)POLARIZED PHOTON CONTENT OF THE NUCLEON

A. MUKHERJEE and C. PISANO
Institüt fur Physik, Universität Dortmund,
D 44221 Dortmund, Germany

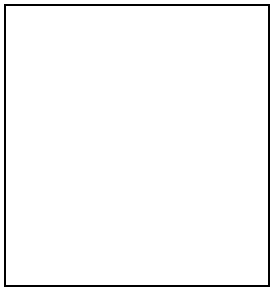

We investigate the QED Compton process (both elastic and inelastic) in unpolarized and longitudinally polarized electron-proton scattering. The cross section can be expressed in terms of the equivalent photon distribution of the proton. We provide the necessary kinematical cuts to extract the photon content of the proton at HERMES and eRHIC. We point out that such a process can give valuable information on $g_1(x_B, Q^2)$ in the small x_B, broad Q^2 region at eRHIC and especially in the lower Q^2, medium x_B region in fixed target experiments.

1 Introduction

QED Compton process (QEDCS) in the scattering $ep \to e\gamma X$ has a distinctive experimental signature: both the outgoing electron and photon are detected at large polar angles and their transverse momenta almost balance each other, with little or no hadronic activity at the detectors [1,2]. QEDCS in unpolarized ep scattering has long been suggested as an excellent channel to measure the structure function $F_2(x_B, Q^2)$ and also to extract the unpolarized photon content of the proton in the equivalent photon approximation (EPA) [1,2,3]. In fact, this has been recently analyzed by members of the H1 collaboration at HERA[4]. Improved kinematical constraints have been suggested in [5,6] for a more accurate extraction of the unpolarized photon distribution. The polarized photon content of the nucleon consists of two components, elastic and inelastic, like its unpolarized counterpart [7,8]. Recently we showed that when the virtuality of the exchanged photon is small, the 'exact' polarized QEDCS cross section is expressed in terms of the polarized equivalent photon distribution of the proton [9]. We gave the necessary kinematical cuts to extract the polarized photon distribution at HERMES and eRHIC by using QED Compton peak; QEDCS can also provide valuable information on $g_1(x_B, Q^2)$ in small Q^2, medium x_B

region at HERMES and over a broad range of x_B, Q^2 at eRHIC. Here we report on our main results.

2 QED COMPTON SCATTERING CROSS SECTION AND THE EPA

We consider the process shown in Fig. 1. X is a generic hadronic system with momentum $P_X = \sum_{X_i} P_{X_i}$. For elastic scattering $P_X = P'$ and X is a proton.

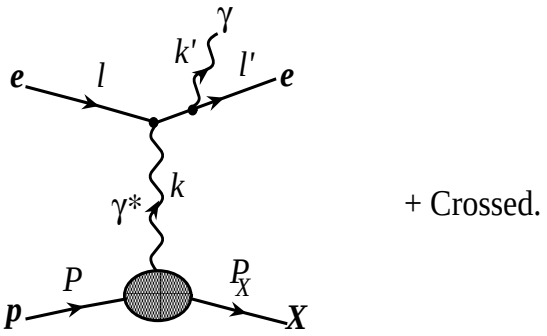

Fig. 1: Feynman diagrams for the QED Compton process (QEDCS). $X \equiv p$ (and $P_X \equiv P'$) corresponds to elastic scattering.

We introduce the invariants

$$S = (P + l)^2, \quad \hat{s} = (l + k)^2, \quad \hat{t} = (l - l')^2, \quad t = k^2, \tag{1}$$

where k is the 4-momentum of the virtual photon. The photon in the final state is real, $k'^2 = 0$. We take the proton mass to be m. The cross section can be calculated in a covariant way [5], both in the elastic and inelastic channels and it can be shown that in the limit $S \gg m^2$ and $\hat{s} \gg |t|$, one can approximate the cross section as

$$\sigma(S) \approx \sigma^{\rm EPA} = \int_{x_{\rm min}}^{(1-m/\sqrt{S})^2} dx \int_{m_e^2-\hat{s}}^{0} d\hat{t}\, \gamma(x, xS)\, \frac{d\hat{\sigma}(xS, \hat{t})}{d\hat{t}}, \tag{2}$$

where $x = \hat{s}/S$ and $\gamma(x, xS)$ is the equivalent photon distribution of the proton [1,2,10,7,8], which has an elastic and an inelastic component; $\frac{d\hat{\sigma}(\hat{s},\hat{t})}{d\hat{t}}$ is the real photoproduction cross section.

When the incident electron and proton are both longitudinally polarized, the cross section in the elastic channel becomes [9]

$$\begin{aligned}
\Delta\sigma_{\rm el} &= \frac{\alpha}{8\pi(S-m^2)^2} \int_{m_e^2}^{(\sqrt{S}-m)^2} d\hat{s} \int_{t_{\rm min}}^{t_{\rm max}} \frac{dt}{t} \int_{\hat{t}_{\rm min}}^{\hat{t}_{\rm max}} d\hat{t} \int_0^{2\pi} d\phi\; X_2^A(\hat{s}, t, \hat{t}) \\
&\quad \times \Bigg[\left(2\,\frac{S-m^2}{\hat{s}-t} - 1 + \frac{2m^2}{t}\frac{\hat{s}-t}{S-m^2} \right) G_M^2(t) \\
&\quad - 2\left(\frac{S-m^2}{\hat{s}-t} - 1 + \frac{m^2}{t}\frac{\hat{s}-t}{S-m^2} \right) \frac{G_M(G_M-G_E)}{1+\tau} \Bigg].
\end{aligned} \tag{3}$$

G_E and G_M are the proton's electric and magnetic form factors and ϕ is the azimuthal angle of the outgoing $e-\gamma$ system in the center-of-mass frame. The limits of integrations follow from kinematics and are the same as in the unpolarized case [5]. $X_2^A(\hat{s}, t, \hat{t})$ can be obtained from the leptonic tensor (see [9] for the definition). The cross section in the inelastic channel is [9]

$$\Delta\sigma_{\rm inel}(S) = \frac{\alpha}{4\pi(S-m^2)^2} \int_{W^2_{\rm min}}^{W^2_{\rm max}} dW^2 \int_{m_e^2}^{(\sqrt{S}-m)^2} d\hat{s} \int_{Q^2_{\rm min}}^{Q^2_{\rm max}} \frac{dQ^2}{Q^2} \frac{1}{(W^2+Q^2-m^2)}$$

$$\times \Big\{\Big[-2\frac{S-m^2}{\hat{s}+Q^2}+\frac{W^2+Q^2-m^2}{Q^2}+\frac{2m^2}{Q^2}\Big(\frac{\hat{s}+Q^2}{S-m^2}\Big)\Big]g_1(x_B,Q^2) + \frac{4m^2}{W^2+Q^2-m^2}g_2(x_B,Q^2)\Big\}\tilde{X}_2^A(\hat{s},Q^2), \quad (4)$$

here $\tilde{X}_2^A(\hat{s},Q^2)=2\pi\int d\hat{t}X_2^A(\hat{s},Q^2,\hat{t})$, W is the invariant mass of the produced hadronic system and $Q^2=-t$. The limits of the integrations are the same as in the unpolarized case and can be found in [5]. When $S\gg m^2$ and $\hat{s}\gg Q^2$, the cross section is approximated to a form similar to (2) with $\gamma(x,xS)$ replaced by $\Delta\gamma(x,xS)$ which is the polarized equivalent photon distribution of the proton and $\frac{d\hat{\sigma}(\hat{s},\hat{t})}{d\hat{t}}$ replaced by $\frac{d\Delta\hat{\sigma}(\hat{s},\hat{t})}{d\hat{t}}$, which is the polarized real photoproduction cross section. $\Delta\gamma(x,xS)$ has both elastic and inelastic components[5,9]. The elastic component of $(\Delta)\gamma$ is expressed in terms of the form factors for which the well-known dipole parametrizations can be used [10,7]. The inelastic component is expressed in terms of the proton structure functions. This component is scale dependent and is our main concern here.

3 NUMERICAL RESULTS

In this section, we show our numerical estimates of the QEDCS process for HERMES and eRHIC kinematics respectively. QEDCS events can be selected by imposing the following constraints on the energies E'_e and E'_γ of the outgoing electron and photon respectively, and on their polar angles θ_e, θ_γ (these constraints are similar to the ones used at HERA for unpolarized scattering):

$$E'_e, E'_\gamma > 4 \text{ GeV}^2$$
$$0.04 \le \theta_e, \theta_\gamma \le 0.2 \quad \text{(HERMES)}; \qquad 0.06 \le \theta_e, \theta_\gamma \le \pi - 0.06 \quad \text{(eRHIC)}$$
$$\hat{s} > 1 \text{ GeV}^2; \quad \hat{s} > Q^2 \quad (5)$$

For HERMES, the incident electron beam energy is $E_e = 27.5$ GeV. For eRHIC, we have taken $E_e = 10$ GeV; $E_p = 250$ GeV. The constraints on the energies and the polar angles of the outgoing particles remove the initial and final state radiative events [1,3] unrelated to QEDCS. The last two cuts basically select the preferable kinematical region where the EPA is expected to hold.

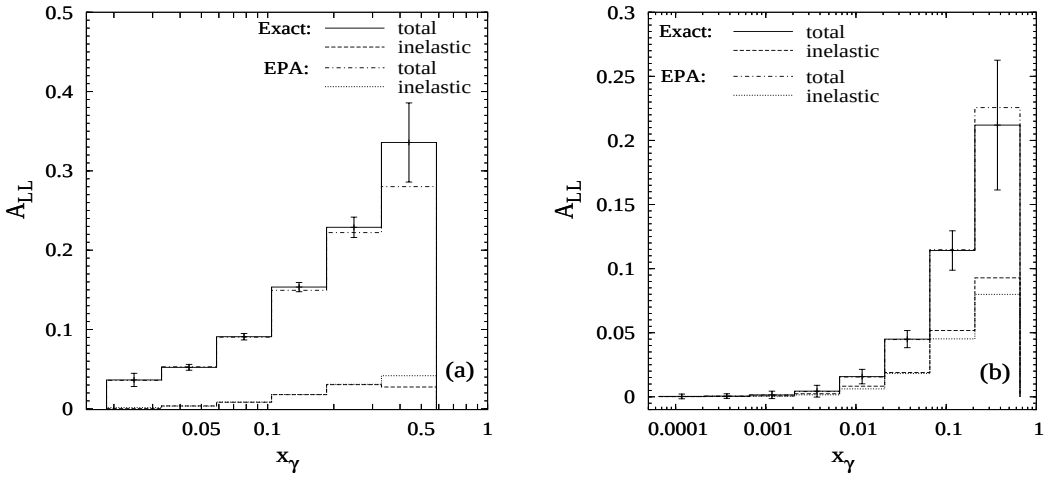

Fig. 2 : (a) Asymmetry in bins of x_γ at HERMES. (b) Asymmetry at eRHIC in bins of x_γ. The constraints imposed are as in (5).

The asymmetry A_{LL} is defined as

$$A_{LL} = \frac{\sigma_{++} - \sigma_{+-}}{\sigma_{++} + \sigma_{+-}} \ , \quad (6)$$

where the indices + and − refer to the helicities of the incident electron and proton respectively. Fig. 2(a) shows the asymmetry for HERMES kinematics in bins of $x_\gamma = \frac{l\cdot k}{P\cdot l}$, which is the fraction of the proton's momentum carried by the photon. In the EPA, $x_\gamma = x$. The total (elastic+inelastic) asymmetry shows an excellent agreement with that calculated in the EPA (shown by the dot-dashed line) in all bins except the last one for higher x_γ. The expected statistical error in each bin is calculated using the formula $\delta A_{LL} \approx \frac{1}{\mathcal{P}_e \mathcal{P}_p \sqrt{\mathcal{L}\sigma_{bin}}}$, where $\mathcal{P}_e$ and $\mathcal{P}_p$ are the polarizations of the incident lepton and proton respectively, $\mathcal{L}$ is the integrated luminosity and $\sigma_{\rm bin}$ is the unpolarized cross section in the corresponding x_γ bin. We have taken $\mathcal{P}_e = \mathcal{P}_p = 0.7$ and $\mathcal{L} = 1 fb^{-1}$ for both HERMES and eRHIC. The asymmetry in the inelastic channel is also shown. The asymmetry is sizable and can give access to the polarized equivalent photon distribution at HERMES. Fig. 2(b) shows the asymmetry for eRHIC. Here events are observed over a broader range of x_γ, however the asymmetry is very small for small x_γ bins, it increases as x_γ increases. As in HERMES, good agreement with the EPA is observed in all but the last bin, where the expected statistical error is also higher due to the smaller number of events.

The cross section receives a major background contribution coming from virtual Compton scattering (VCS), when the final state photon is emitted from the proton side. Particularly important is the inelastic VCS, because it affects the determination of the inelastic component of $(\Delta)\gamma$. The inelastic VCS was estimated in [6,9] in an 'effective' parton model (also valid at low Q^2). It was observed that both the polarized and unpolarized VCS contributions are suppressed in the region $\hat{s} < \hat{S}$ where $\hat{S} = \frac{\hat{t}(x_l - x_B)}{x_l}$ with $x_l = \frac{-\hat{t}}{2P\cdot(l-l')}$. Both $\hat{s}$ and $\hat{S}$ are measurable quantities. The interference between QEDCS and VCS was found to be suppressed in this region at eRHIC but not so much at HERMES. However, it changes sign when a positron beam is used instead of the electron beam, a combination of electron and positron scattering data can eliminate this contribution.

Finally, we point out that such an experiment can provide valuable information on the spin structure function $g_1(x_B, Q^2)$ in a kinematical region not well-covered by fully inclusive experiments (in fact, the unpolarized structure function $F_2(x_B, Q^2)$ has been measured by measuring QED Compton peak at HERA [4,11]) because of its different kinematics compared to inclusive deep inelastic scattering. $g_1(x_B, Q^2)$ can be accessed especially at low Q^2, medium x_B region at HERMES and over a very broad x_B, Q^2 range at eRHIC using the QED Compton process [9].

Acknowledgements

We warmly acknowledge E. Reya and M. Glück for initiating this study, as well as for many fruitful discussions. AM thanks the organizers of the 39 th Rencontres de Moriond session on QCD and High Energy Hadronic Interactions for a wonderful and stimulating workshop. This work has been supported in part by the 'Bundesministerium für Bildung und Forschung', Berlin/Bonn.

References

1. J. Blümlein, G. Levman, H. Spiesberger, *J. Phys. G* **19**, 1695 (1993) .
2. A. De Rujula, W. Vogelsang, *Phys. Lett.* B **451**, 437 (1999).
3. A. Courau and P. Kessler, *Phys. Rev.* D **46**, 117 (1992).
4. V. Lendermann, H. C. Schultz-Coulon, D. Wegener, *Eur. Phys. J. C* **31**, 343 (2003).
5. A. Mukherjee, C. Pisano, *Eur. Phys. J. C* **30**, 477 (2003).
6. A. Mukherjee, C. Pisano, hep-ph/0402046, to appear in *Eur. Phys. J. C.*
7. M. Glück, C. Pisano, E. Reya, *Phys. Lett.* B **540**, 75 (2002).

8. M. Glück, C. Pisano, E. Reya, I. Schienbein, *Eur. Phys. J. C* **27**, 427 (2003).
9. A. Mukherjee, C. Pisano, hep-ph/0405079.
10. B. Kniehl, Phys. Lett. **B 254**, 267, (1991).
11. V. Lenderman, Ph. D. thesis, Univ. Dortmund, H1 collaboration, DESY-THESIS-2002-004, (2002).